Research papers

Spatial-temporal variations in evapotranspiration across the continental United States: An atmospheric water balance perspective

Shasha Shang [a], Gaofeng Zhu [b,*], Kun Zhang [c], Huiling Chen [d], Yidong Wang [a,e], Yang Chen [a], Zhenyu Zhang [f], Ning Ma [g,**]

[a] Tianjin Key Laboratory of Water Resources and Environment, Tianjin Normal University, Tianjin, China
[b] College of Earth and Environmental Sciences, Lanzhou University, Lanzhou, China
[c] School of Geospatial Engineering and Science, Sun Yat-sen University, Zhuhai, China
[d] College of Geography and Environmental Sciences, Zhejiang Normal University, Jinhua, China
[e] School of Geographic and Environmental Sciences, Tianjin Normal University, Tianjin, China
[f] Institute of Meteorology and Climate Research (IMK-IFU), Karlsruhe Institute of Technology, Campus Alpin, Garmisch-Partenkirchen, Germany
[g] Key Laboratory of Water Cycle and Related Land Surface Processes, Institute of Geographic Sciences and Natural Resources Research, China Academy of Sciences, Beijing, China

ARTICLE INFO

ABSTRACT

Accurate estimation of terrestrial evapotranspiration (ET) is crucial for understanding land–atmosphere interactions, but is challenging on the regional scales. The water balance approach, including terrestrial and atmospheric water balance (TWB and AWB), provides a simple tool for estimating regional ET. This study estimated ET values based on the AWB approach (ET_{AWB}) over the continental United States (CONUS) for the period 1979–2021. Validations using TWB-based ET estimates (ET_{TWB}) suggest that ET_{AWB} is accurate. ET_{AWB} demonstrates comparable interannual variability with the other three long-term ET products over the CONUS and is consistent with ET_{TWB} in the majority of basins. The 43-year CONUS averaged ET_{AWB} is 548 ± 26 mm/year, with higher values in the eastern region and the coastal regions in the western CONUS, and lower values in the western arid regions. During 1979–2021, increasing trends of ET_{AWB} are observed in the eastern CONUS, while decreasing trends occurred in the western regions. The intercomparison between ET_{AWB}, GLEAM, Noah, and ERA5 illustrates similar spatial patterns and linear trends. In the water-limited arid basins, ET_{AWB} anomalies over time show strong agreements with precipitation anomalies. The results of this study indicate that the AWB approach provides reasonable regional-to-continental terrestrial ET estimates over the CONUS, serving as a reference for hydrological and climatic modeling.

1. Introduction

Evapotranspiration (ET) is one of the most important fluxes in the Earth's climate system, exchanging water, carbon, and energy between the atmosphere and the land surface (Oki & Kanae, 2006; Trenberth et al., 2009), thereby linking the land and atmospheric branches of the hydrological cycle. More than 60% of precipitation on the land surface is returned to the atmosphere through ET, while also consuming over 50% of the solar radiation at the land surface. Consequently, ET strongly influences atmospheric water vapor transport patterns and the terrestrial water availability, which are essential for regulating the climate.

Therefore, accurate estimation of ET is critical for enhancing our understanding of atmosphere-hydrosphere interactions and for effectively managing water resources.

Traditionally, ET is monitored using *in situ* measurements such as lysimeters, Bowen ratio energy balance and eddy covariance ([EC]) (Allen et al., 2011). However, such ground-based measurements are costly and time-consuming, especially when the regional scale (large areas with various sizes and shapes) is of interest (Xu & Singh, 2005). Consequently, estimating regional-scale ET relies on modeling techniques. Models used to estimate ET are broadly categorized into land surface models (LSMs) (Ma et al., 2017; Mu et al., 2011; Xia et al., 2016;

Zhang et al., 2022), remote sensing-based models (RSMs) (Ma & Zhang, 2022; Yu et al., 2022; Zhang et al., 2019), data assimilation systems (Lu et al., 2017), the complementary relationship (CR) (Ma et al., 2020; Ma & Szilagyi, 2019; Szilagyi & Jozsa, 2018), upscaling of ground ET measurements (Jung et al., 2019), reanalysis (Gelaro et al., 2017; Hersbach et al., 2020; Kobayashi et al., 2015), process-based ecosystem models such as TRENDY (Liu et al., 2021a), and the Coupled Model Intercomparison Project Phase 6 (Liu, et al., 2021b). These models aim to represent and predict the spatiotemporal variability of ET from the regional scale to the global scale. However, most of the available ET products mentioned above rely on input parameters related to soil and vegetation, leading to additional uncertainties due to some assumptions (Martens et al., 2017a; Masson et al., 2003; Mu et al., 2011). LSMs are directly constrained by soil moisture availability (Long et al., 2014; Yang et al., 2013), which may accumulate errors and amplify uncertainties in ET simulations. Spatial resolution mismatch among forcing data exists in RSMs, such as finer vegetation data and coarser meteorological data (Yang et al., 2013). Data assimilation techniques combine the advantages of model simulation and remote sensing techniques, but the uncertainty of the data involved in the assimilation process may impair their performance (Zou et al., 2017). Although the CR model requires only routine meteorological variables, it has certain difficulties in estimating ET at high temporal (e.g., hourly) and spatial (e.g., a few hundred meters) resolutions (Ma et al., 2021; Szilagyi et al., 2017). The upscaling method is also constrained by the availability and quality of data (Liu et al., 2016). Reanalysis products typically exhibit inherent biases and uncertainties due to the assimilation process, particularly in regions with sparse observational data. Therefore, a large-scale assessment of different ET products by direct or indirect evaluation methods is required for their use in global and regional hydrological studies (Shao et al., 2022).

The global FLUXNET networks are commonly used to assess the ET products at various time series across different vegetation types (Chen et al., 2020; Liu et al., 2023; Volk et al., 2023; Zhang et al., 2019). However, its utility for evaluation is limited due to the relatively short period, sparse spatial coverage, and the lack of energy balance closure at some EC sites. Alternatively, the water-balanced approach, including terrestrial water balance (TWB) and atmospheric water balance (AWB), provides a check for the modeled ET products (Builes-Jaramillo & Poveda, 2018) and is also the simplest tool for estimating regional ET. In theory, ET can be expressed as the residual between precipitation (P) minus the sum of net runoff (S) and terrestrial water storage (TWS) change at the basin scale (Pascolini-Campbell et al., 2020; Rodell et al., 2004). Numerous studies have estimated ET at the basin scale based on TWB to serve as a reference for the modeled ET (e.g., Chen et al., 2020; Liu et al., 2016; Ma & Szilagyi, 2019; Zhang et al., 2022). However, most of these studies have been limited to basin scales from 10^{-1} km^2 to 10^3 km^2 and have seldom been applied to a larger scale for estimating ET values. Additionally, due to the paucity of data with adequate resolution and enough length, for example, the period of Gravity Recovery and Climate Experiment (GRACE) water storage only starts from 2002, discharge measurements are often unavailable due to technical or political reasons, and the significant spatial resolution difference between the GRACE and the ET products, the TWB approach tends to result in many uncertainties in small basins (Longuevergne et al., 2010; Ma & Szilagyi, 2019).

Another approach to estimating ET using the water balance method is the AWB, derived as the residual of precipitation (P), atmospheric water vapor convergence ($-\nabla \cdot Q$), and atmospheric water storage change ($\frac{\partial W}{\partial t}$) (Oki et al., 1995). The calculation of atmospheric water-balanced ET (ET$_{AWB}$) relies on detailed meteorological information, including winds and humidity, usually derived from radiosondes and complemented by remote sensing techniques and atmospheric analysis models to achieve a steady and time-continuous global coverage. Using abundant aerological data to estimate ET offers a way to overcome the

issues of unsatisfactory runoff data in the TWB approach, providing another direct method to verify model simulations. However, the AWB is commonly used to analyze the atmospheric water budget related to precipitation change under climate change from an atmospheric perspective (Dagan et al., 2019; Shang et al., 2022; Su & Smith, 2021). Serving as a link between the terrestrial and the atmospheric hydrological cycle, ET is the total water vapor flux transported from the surface to the atmosphere. This is considered terrestrial ET whether it is part of the atmospheric water balance or the terrestrial water balance. However, few studies shed light on estimating terrestrial ET from the perspective of the AWB, despite ET being one of the most important links between both the terrestrial and atmospheric branches of the hydrological cycle.

Previous studies have attempted to estimate regional ET using the AWB approach over the continental United States (CONUS) (RASMUSSON, 1968; RASMUSSON 1971; Ropelewski and Yarosh, 1998; Yeh et al., 1998). For example, Yeh et al. (1998) demonstrated that the regional ET can be statistically estimated by the AWB approach at a scale similar to that of Illinois through a comparison of the ET estimates from AWB and soil water balance. However, due to the scarcity of ground measurements data, the limited temporal-spatial resolution, and the short period for the atmospheric reanalysis (e.g., specific humidity, wind speed), the validation of the atmospheric water balanced ET estimates over the CONUS in the previous literature is limited (Yeh et al., 1998). With the increase in ground observations and advancements in remote sensing and atmospheric analysis models, such as the European Center for Medium-Range Weather Forecasts Reanalysis (ERA5), which has been demonstrated as one of the best-performing reanalysis in many studies (Hersbach et al., 2020; Tarek et al., 2020), more refined materials are available for estimating ET using the AWB approach.

Therefore, the objectives of this study are 1) to estimate ET over the CONUS based on the AWB approach using observed precipitation data and ERA5 reanalysis, producing a set of the atmospheric water-balanced ET product at a daily scale during 1979–2021; 2) to investigate the validity of the AWB computations for the regional-scale ET estimates by comparing them with TWB-based ET estimates at the basin scale and mainstream global gridded ET products over the CONUS; and 3) to analyze the spatial–temporal variations in evapotranspiration over the CONUS based on the AWB approach. Once validated, the AWB-based ET estimates can serve as a reference for modeled regional ET and climate simulations.

2. Materials and methods

2.1. Atmospheric water balance

The atmospheric water balance equation can be written as follows (Oki et al., 1995):

$$\frac{\partial W}{\partial t} = -\nabla \cdot Q + ET - P \tag{1}$$

where $\frac{\partial W}{\partial t}$ is the change of atmospheric water storage, $-\nabla \cdot Q$ is the mean convergence of the horizontal atmospheric water vapor fluxes, ET is the evapotranspiration, and P denotes the precipitation.

The atmospheric water-balance-based evapotranspiration (ET_{AWB}) can be derived by solving equation (1) for ET using observed precipitation, the atmospheric water vapor storage change, and the vertically integrated atmospheric moisture convergence as:

$$ET_{AWB} = P + \nabla \cdot Q - \frac{\partial W}{\partial t} \tag{2}$$

in this study, the ET_{AWB} is calculated on a daily scale at a 0.25° resolution from 1979 to 2021 and converted to monthly data for comparison. The CPC Unified Gauge-Based Analysis of daily precipitation (Chen & Xie,

2008; Xie et al., 2010) over the CONUS with a 0.25° resolution is used to calculate the daily ET. The quality of the CPC precipitation data has been evaluated by Chen et al., (2008) which indicates that the optimal interpolation (OI) technique used to generate CPC precipitation product shows stable performance statistics over the CONUS. The ERA5 reanalysis (Hersbach et al., 2020)) provides the hourly vertical integrated moisture convergence and the total column atmospheric water vapor with a 0.25° resolution. The ERA5 reanalysis is the most recent reanalysis dataset of ECMWF which combines vast amounts of historical observations into global estimates from 1950 onwards and replaces the ERA-Interim dataset. There are pronounced improvements and changes from ERA-Interim to ERA5 in the assimilation scheme, observation system, and model algorithm. The spatial resolution of ERA5 has been increased to ~ 31 km (0.25°) with 137 vertical layers and hourly output. The improved temporal and spatial resolution allow for a detailed evolution of weather systems. The variable of the total amount of water vapor in a column from ERA5 extends from the surface of the earth to the top of the atmosphere which represents the area averaged value for a grid box.

2.2. Terrestrial water balance

The basin-scale TWB-based evapotranspiration (ET_{TWB}) can be derived as:

$$ET_{TWB} = P - R - \frac{\partial S}{\partial t} \qquad (3)$$

where P, R, and $\frac{\partial S}{\partial t}$ represent the basin-wide precipitation, stream runoff, and terrestrial water storage change respectively.

In this study, we estimated the TWB-based ET (ET_{TWB}) of 18 first-level two-digit (i.e., HUC2) hydrological units (Fig. 1) in the CONUS (Seaber et al., 1987) on an annual scale. The evaluations of ET at the basin scale are based on basin-wide ET averaged over the 18 basins. Basic information on 18 river basins employed in this study is summarized in Supplementary Table 1. Since the TWS datasets from the GRACE (Tapley et al., 2019) are only available from 2002, the yearly TWS data from 1980 to 2002 are from GRACE-REC (Humphrey & Gudmundsson, 2019). The GRACE-REC product is a state-of-the-art climate-driven TWS product trained by a statistical model. It provides a century-long reconstruction including the pre-GRACE period, which has become popular for long-term hydro-climatological studies. In this study, the JPL Mascon RL06.1 Version 3.0 GRACE data are employed in Equation (4) to calculate ET at the basin scale. Meanwhile, the GRACE-

REC version used in the study was forced by ERA5 precipitation and temperature data and calibrated by mascons from the Jet Propulsion Laboratory (JPL).

The basin-wide runoff from 1979 to 2020 for all hydrological units is sourced from the United States Geological Survey (USGS). The annual precipitation is also integrated from the CPC Unified Gauge-Based Analysis of daily precipitation in the TWB.

2.3. Long-term gridded terrestrial ET products

In this study, we selected three main-stream long-term ET products including the Global Land Evapotranspiration Amsterdam Model (GLEAM), NLDAS Noah Land Surface Model and ERA5 to provide a performance comparison for the ET_{AWB}. These three products were chosen because they have identical temporal coverage to the ET_{AWB}. Other products, such as Complementary relationship (CR) model (Ma et al. 2021), the FLUXNET-MTE (Jung et al., 2011) and the Peman-Monteith-Leuning (PML) data (Zhang et al., 2017) have shorter period. GLEAM is designed to be driven solely by remote sensing observations. In the present study, we used the GLEAM V3.6a, covering the period from 1980 to 2021 on a daily time step at a 0.25° resolution, which was then converted to a monthly scale (Martens et al., 2017b). The Noah land surface model was driven by NLDAS-2 atmospheric forcing at a 0.125° resolution, generating monthly data for a series of land surface parameters (accumulation of rainfall, snowfall, subsurface runoff, surface runoff, and total evapotranspiration) from 1979 to the present (Xia et al. 2012). All products were remapped to 0.25° using bilinear interpolation.

Five statistical metrics were used in this study: (1) coefficient of determination (R^2), (2) root-mean-square error (RMSE), (3) mean absolute error (MAE), (4) Nash-Sutcliffe efficiency coefficient (NSE), (5) correlation coefficient (R).

3. Results

3.1. Validation of ET_{AWB} at the basin scale

Fig. 2 presents the scatter plot of the linear regression between the ET_{AWB}, GLEAM, Noah, and ERA5 against the ET_{TWB} for the 18 HUC2 basins over the CONUS. Both the ET_{AWB} and the other three products display relatively good consistency with the ET_{TWB}, with the R^2 ranging from 0.864 to 0.962 (ET_{AWB} is 0.929) and NSE values close to 1 (ET_{AWB} is 0.784). Compared to the other three ET products, the RMSE of ET_{AWB} is 99.299, only slightly higher than that of Noah. The linear regression
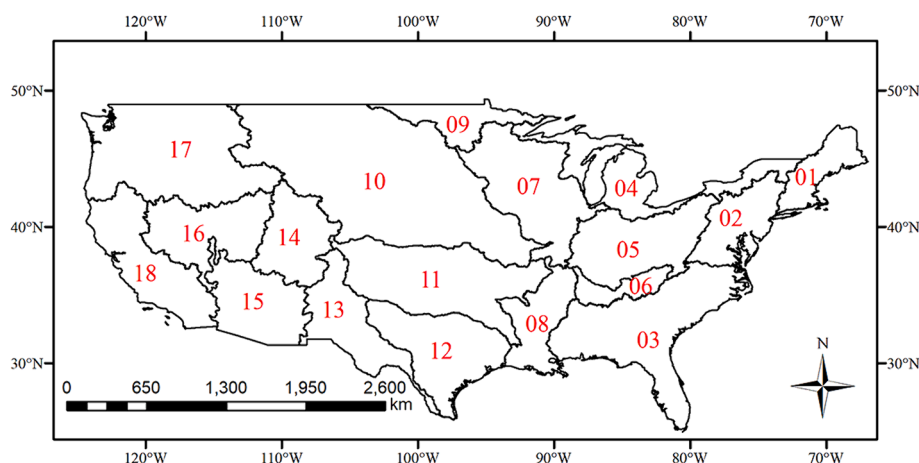

Fig. 1. Location of 18 HUC2 basins across the CONUS (01 = New England, 02 = Mid-Atlantic, 03 = South Atlantic-Gulf, 04 = Great Lakes, 05 = Ohio, 06 = Tennessee, 07 = Upper Mississippi, 08 = Lower Mississippi, 09 = Souris-Red-Rainy, 10 = Missouri, 11 = Arkansas-White-Red, 12 = Texas Gulf, 13 = Rio Grande, 14 = Upper Colorado, 15 = Lower Colorado, 16 = Great Basin, 17 = Pacific Northwest, 18 = California). (For interpretation of the references to colour in this figure legend, the reader is referred to the web version of this article.)
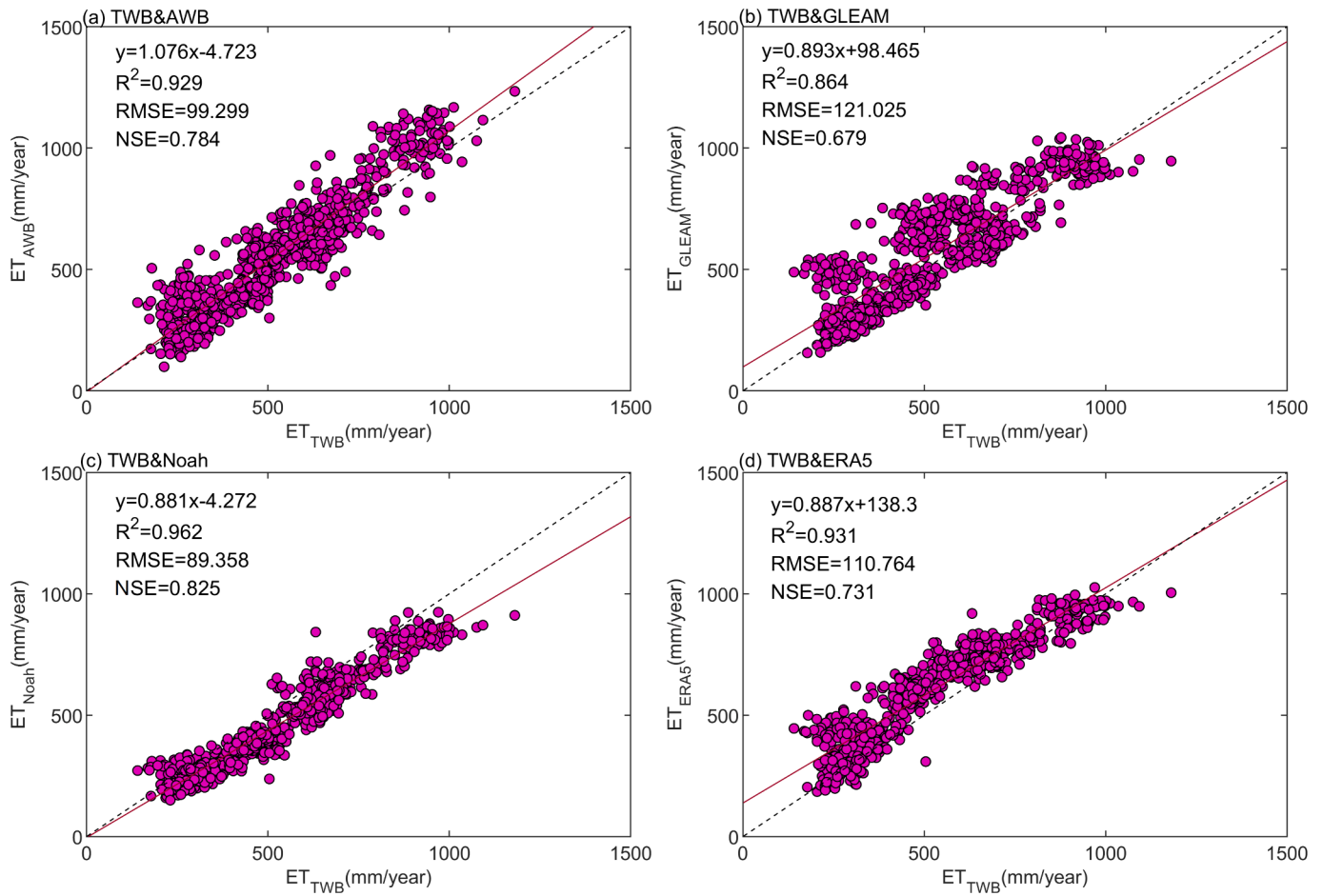
Fig. 2. Regression plots of the annual ET_{AWB}, GLEAM, Noah and ERA5 against the ET_{TWB} at 18 HUC2 basins during their overlapping temporal coverage from 1979 to 2021. The black dashed lines represent the 1:1 line and the magenta lines are the regression line. RMSE is in the unit of mm/year. (For interpretation of the references to colour in this figure legend, the reader is referred to the web version of this article.)

slope between the ET_{AWB} and ET_{TWB} is 1.076, indicating a tendency to overestimate high values of ET_{TWB}, while the GLEAM and Noah tend to underestimate, particularly Noah. However, GLEAM and ERA5 tend to overestimate low values of the ET_{TWB}. The results of the regression plot of the annual ET_{AWB}, GLEAM, Noah and ERA5 against the ET_{TWB}, calculated from GRACE during the period 2002–2020, also shows similar findings (Figure S1).

Fig. 3 further displays the evaluation of the annual ET_{AWB} and the other three ET products against the ET_{TWB} at 18 basins. ET_{AWB} shows good consistency with the ET_{TWB}, with R^2 values higher than 0.8 at all the basins. NSE values for ET_{AWB} are close to 1, except for the Upper Colorado, which has values lower than 0.5, similar to GLEAM and ERA5. Noah and ERA5 shows the highest consistency with ET_{TWB}, with R^2 exceeding 0.9 in all most all basins, whereas GLEAM demonstrates the lowest consistency. The MAE values from the ET_{AWB} are lower than 100 mm/year at most basins, which is comparable to the other three mainstream products. Compared to the other three products, ET_{AWB} shows a relatively lower deviation at most basins in terms of the RMSE. Overall, ET_{AWB} closely agrees with the ET_{TWB} in the 18 HUC2 basins over the CONUS. This indicates that ET_{AWB} is reasonable for reproducing the estimation of ET at basin scales.

To evaluate the performance of the ET_{AWB} to capture the interannual variations in long time series, the comparison for interannual variability of the annual ET_{AWB}, GLEAM, Noah, ERA5 and ET_{TWB} at 18 HUC2 basins over the CONUS is shown in Fig. 4. It is found that the interannual variation of the ET_{AWB} is consistent with that of the ET_{TWB} at the majority of the basins over the CONUS. The consistency is the highest in the

Souris-Red-Rainy (Basin 09), the Missouri (Basin 10), the Arkansas-White-Red (Basin 11), the Rio Grande (Basin 13), the Upper Colorado (Basin 14), and the Lower Colorado (Basin15) with correlation coefficients all exceeding 0.65 and being significant at the 99 % confidence level (Table S2). Noah also shows better performance in capturing the interannual variability in basins 09 to 15, similar to the ET_{AWB}. However, the magnitude of Noah is always the lowest among the four products, which underestimates the ET_{TWB} at almost all the HUC02 basins and shows the smallest interannual variability. In contrast, GLEAM is not performing well in capturing the interannual variability in HUC2 basins. ERA5 usually overestimates the ET values compared to ET_{TWB}.

3.2. Spatial-temporal patterns in ET over the CONUS

Figure 5 shows the spatial distribution of the muti-year (1979–2021) mean annual ET_{AWB}. ET_{AWB} shows higher values over the humid regions in the eastern CONUS and lower values over the arid regions in the western CONUS. The highest ET value was observed in the southeastern CONUS (>1000 mm/year) and also over the Great Salt Lake, since the AWB approach does not only focus on land surface ET. In addition, high ET estimates also occurred over the coastal regions in western CONUS, which receive much of the annual precipitation in the form of orographic heavy rain (Gershunov et al., 2019). The spatial pattern of the multi-year mean annual ET_{AWB} is consistent with that of the mainstream ET products (Figure S2), except for the magnitude of ET values in the Gulf Coastal Plain and Florida peninsula, which are
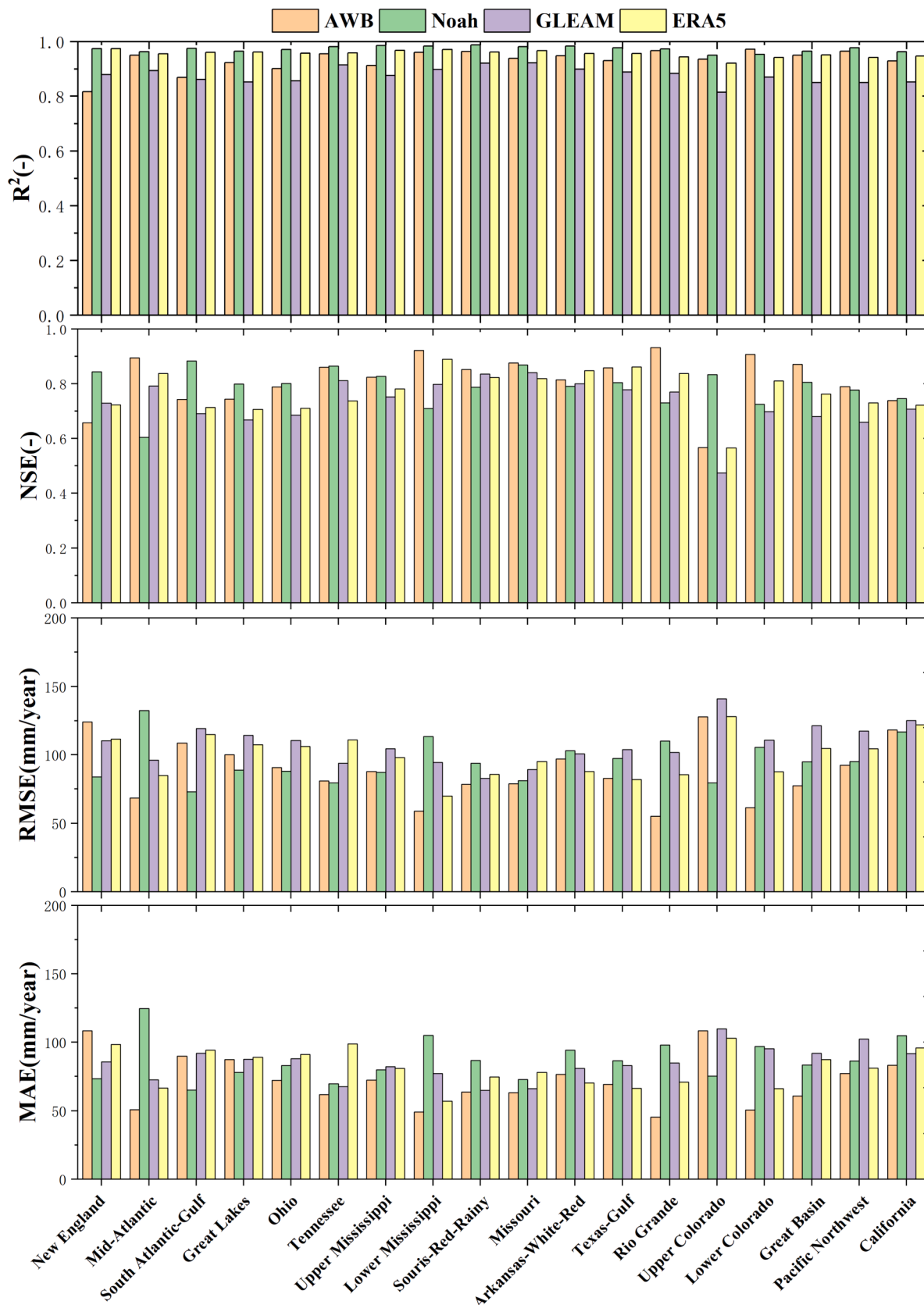
Fig. 3. Comparison of the estimated ET from the AWB approach and the other three products versus the ET_{TWB} at 18 HUC2 basins over the CONUS.
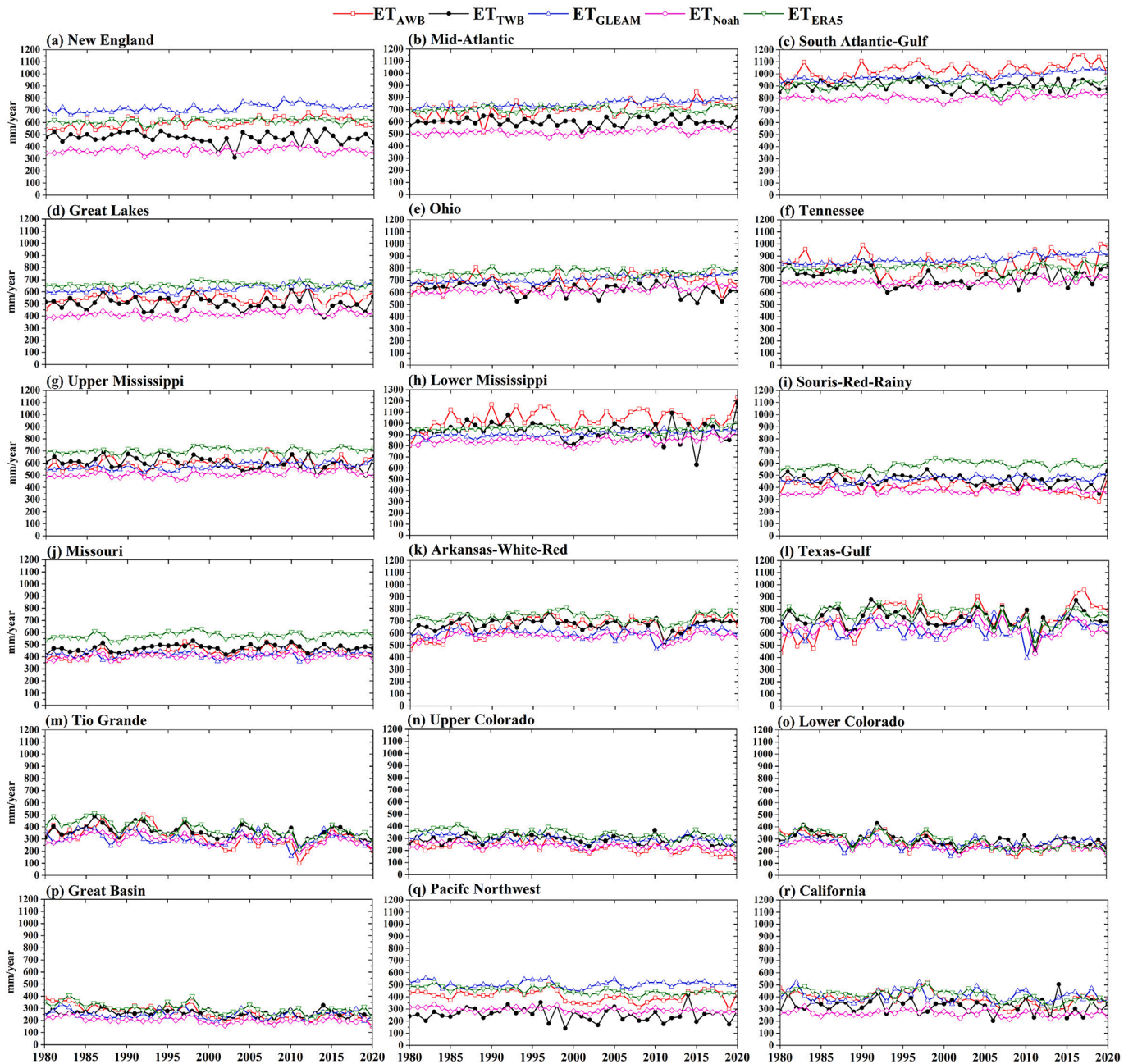
Fig. 4. Time series of mean annual ET based on AWB, GLEAM, Noah, ERA5, and TWB approach at 18 HUC2 basins over the CONUS.
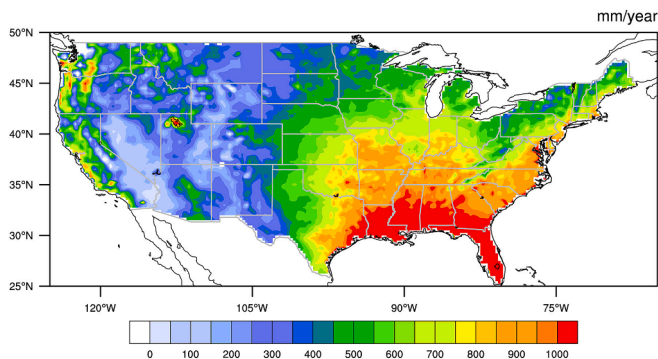

Figure 5. Spatial pattern of the multi-year mean annual ET_{AWB} from 1979 to 2021.

estimated to be higher than in the other three products. Figure 6 shows the time series of the CONUS-averaged ET_{AWB} and ET estimates from GLEAM, Noah, and ERA5. ET_{AWB} shows comparable interdecadal variability to GLEAM (R=0.63, p < 0.01), Noah (R=0.59, p < 0.01), and ERA5 (R=0.52, p < 0.01). The values of annual ET_{AWB} are close to that of GLEAM, higher than Noah's and lower than ERA5. The CONUS-averaged multiyear mean annual ET estimated by ET_{AWB}, GLEAM, Noah and ERA5 are 548 ± 26 mm/year, 544 ± 18 mm/year, 455 ± 12 mm/year, and 603 ± 20 mm/year. The results indicate that the performance of the CONUS-regional-averaged ET_{AWB} is reasonable at the regional scale compared to mainstream gridded ET products.

Fig. 7 shows the 43-year-averaged (1979–2021) seasonal cycle of ET_{AWB} and the other AWB components (i.e., precipitation, atmospheric moisture convergence, and atmospheric water vapor storage change) over the CONUS. Overall, ET_{AWB} estimates show a comparable seasonal cycle to the other three mainstream products (**Figure S3**), with maxima
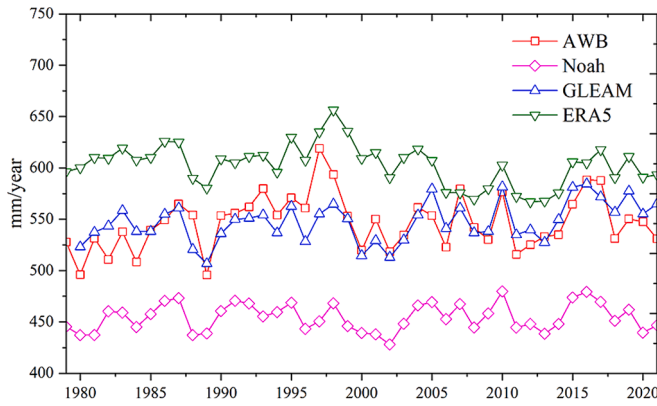
Figure 6. Time series of the annual ET$_{AWB}$ and ET estimates from the other three products.
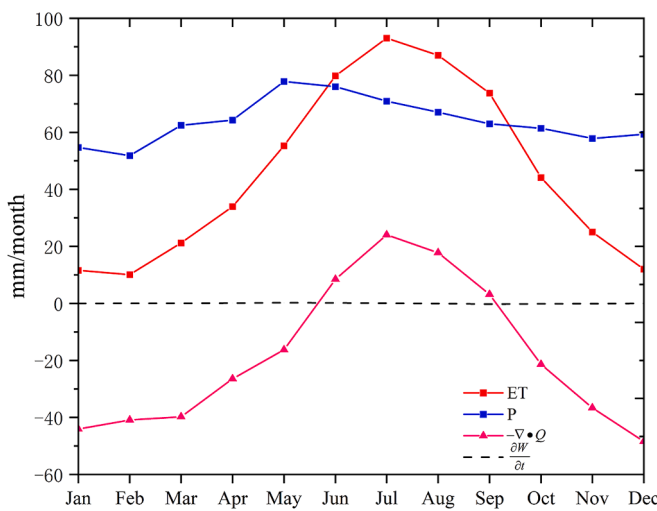

Fig. 7. Seasonal cycle of the atmospheric water balance components in CONUS. Here P is precipitation, ET is the evapotranspiration estimate from the AWB, $-\nabla \cdot Q$ represents the atmospheric moisture convergence, and $\frac{\partial W}{\partial t}$ denotes the change in the atmospheric water storage.

in the summer (June-July-August) and minimum in the winter (December-January-February) although with a relatively higher magnitude in the summer for ET$_{AWB}$. Additionally, ET$_{AWB}$ shows a higher value in September (75 mm/month) compared to GLEAM, Noah and ERA5 (50–60 mm/month), resulting in high ET values lasting for four months in ET$_{AWB}$. ET values from Noah are smaller than those from GLEAM from January to July, suggesting that the underestimation of Noah may be due to the underestimates in these months. However, ERA5 is overestimated in May, June, July, August, and September. The seasonal cycle of the AWB components averaged over the entire CONUS shows that the seasonal cycle of precipitation is not significant. During June, July, August, and September, ET values exceed that of precipitation, while precipitation is much larger than ET during winter months. The seasonal cycle of atmospheric moisture convergence is similar to that of ET$_{AWB}$. The monthly moisture convergence values are positive in June, July, August, and September, indicating net water vapor input during these periods while divergence away from this region during the remaining months of the year. The change in atmospheric water storage is negligible.

Fig. 8 the seasonal cycle of the ET$_{AWB}$ and the other AWB components at the 18 HUC2 basins to assess the performance of the AWB approach in capturing the seasonal cycle of ET in different climate zones. Table S3 summarizes the climate types of 18 HUC2 basins are according

to the Köppen climate classification system (Beck et al., 2018). Basins 01 to 06 mainly belong to the humid continental and subtropical climate characterized by hot and wet summers. Therefore, high ET values in June, July, August, and September with a magnitude higher than 100 mm/month are observed, which is more or less equivalent to the CONUS-average value. Basin 07, 08, and 09 demonstrate a peak value in July influenced by monsoon. The values of ET, precipitation, and moisture convergence in Basin 13, 14, and 15 are relatively low due to their semi-arid climates. Basins 17 and 18 (especially Basin 18) show comparable ET values every month, while precipitation shows an "inverted V" due to the Mediterranean climate's characteristics of mild wet winters and warm to hot dry summers. These results indicate that ET$_{AWB}$ reasonably captured the characteristics of the seasonal cycle in different climate zones over the CONUS.

3.3. Long-term trends of ET in the CONUS from 1979 to 2021

Fig. 9 displays the spatial pattern of the estimated linear trends in ET$_{AWB}$ over the CONUS from 1979 to 2021 showing a significant decrease in the western CONUS and a significant increase on the eastern coast and the Gulf Coast. Overall, the spatial distribution of the linear trends in ET$_{AWB}$ is roughly consistent with GLEAM, Noah, and ERA5, showing negative trends in the western CONUS and positive trends in the eastern CONUS, although the positive trends in ERA5 are not as significant (Figure S4). The magnitude of the increasing trend in ET$_{AWB}$ over the eastern CONUS is closer to ERA5. However, a decreasing trend occurred in the State of Minnesota, the Appalachian Mountains in the ET$_{AWB}$, which is inconsistent with Noah and GLEAM.

Fig. 10 further shows the anomaly values of annual ET$_{AWB}$ and CPC precipitation averaged over the CONUS from 1979 to 2021. The anomalies are defined as the annual average value of ET and precipitation every year minus the average multi-year mean value from 1979 to 2021. It is shown that ET anomalies track precipitation anomalies from the end of the 1900s averaged across the entire CONUS, indicating precipitation is more likely lost to ET during that period. To investigate the correlations of the ET and precipitation in different regions, Fig. 11 displays the anomaly values of the annual ET and precipitation averaged in the 18 HUC2 basins, respectively. The anomalies of the ET and precipitation are particularly consistent in the Rio Grande (Basin 13), Upper Colorado (Basin 14), Lower Colorado (Basin 15), and the Great Basin (Basin 16), where ET amounts are less than 30 mm/month, with the correlation coefficient values larger than 0.75 and statistically significant at the 99% confidence level (Fig. 5). This is because the ET in these arid regions being water-limited, leading to a larger fraction of precipitation being lost to ET, which in turn causes the ET anomalies to track the precipitation anomalies more closely. However, the situation is different in humid regions because ET tends to be energy-limited, as concluded in other studies using different types of ET products (Hamlet et al., 2007; T. Xu et al., 2019).

4. Discussion

4.1. Comparison of ET$_{AWB}$ with other ET products

The estimation of ET$_{AWB}$ in the present study reasonably captured the spatial–temporal pattern and trends of the ET over the CONUS reasonably compared to other products (Figures 5 and 9 and Figures S1 and S2) and results from previous studies (Ma & Szilagyi, 2019; Reitz et al., 2023; Velpuri et al., 2013; Ma et al., 2024). ET$_{AWB}$ exhibits high values in the eastern CONUS and the coastal region of the western CONUS due to its pattern tracking the precipitation pattern (Cui et al., 2017; Gershunov et al., 2019; Koster et al., 2015; Portmann et al., 2009). Regarding the magnitude, Noah tends to underestimate ET values over the CONUS (Figure 6, FigureS1) compared to other products, as observed in other studies (Ma & Szilagyi, 2019; Xia et al., 2016). In contrast, ERA5 estimated higher values over the CONUS (Figures 6).
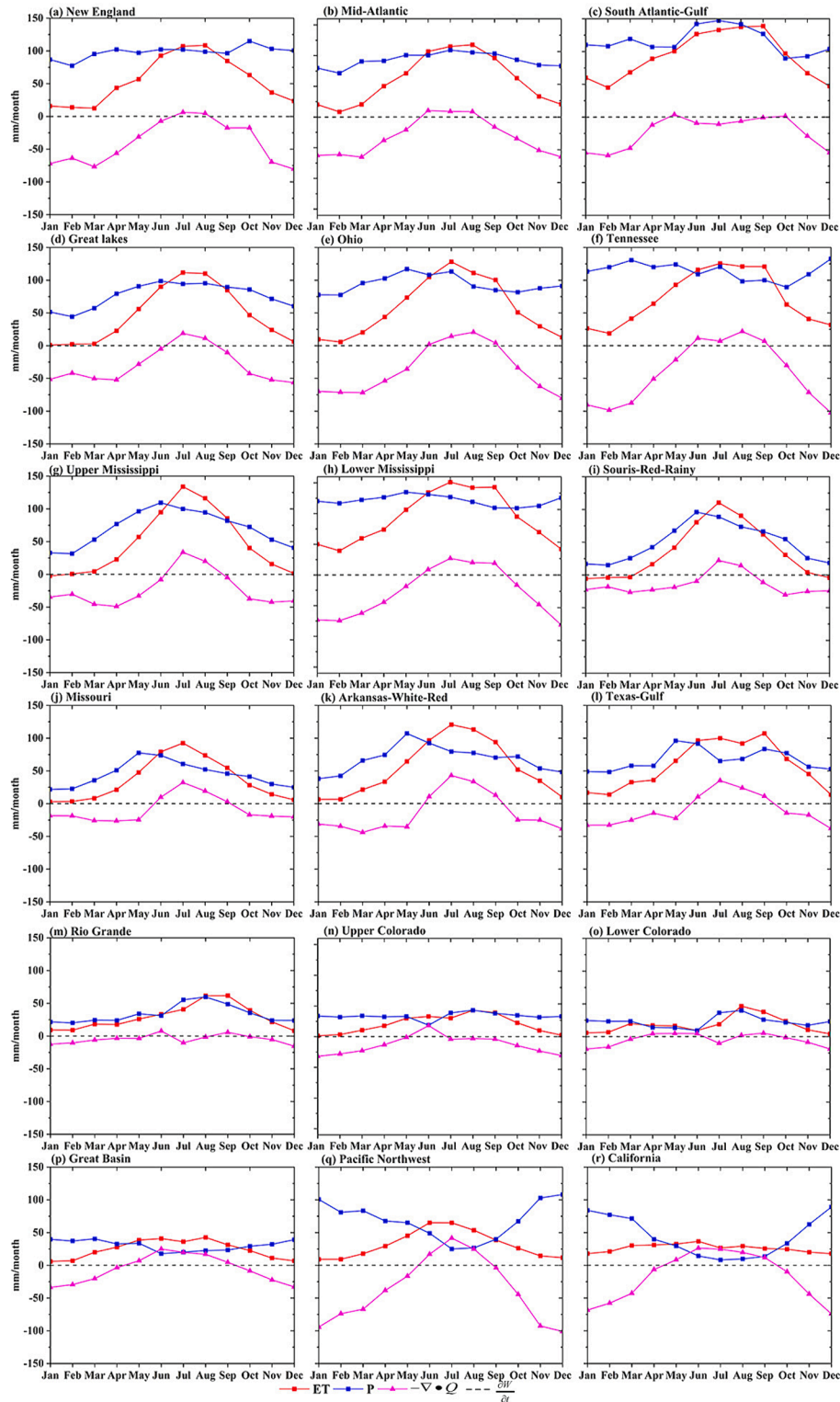
Fig. 8. Seasonal cycle of the atmospheric water balance components of 18 HUC2 basins respectively. Here P represents precipitation, ET represents the evapo-transpiration estimated from the AWB approach, $-\nabla \cdot Q$ represents the atmospheric moisture convergence, and $\frac{\partial W}{\partial t}$ denotes the change in the atmospheric water storage.

Model intercomparisons in previous studies have also indicated that reanalysis-based ET is much higher than that from LSM and RSM-based products (Miralles et al., 2016; Mueller et al., 2013). The regression of the ET_{AWB}, Noah, GLEAM, and ERA5 against the ET_{TWB} indicates that Noah performs the best, followed by ERA5, with GLEAM performing the worst (Fig. 2). This may be because only Noah is intended exclusively for

the CONUS, providing more reliable atmospheric forcing, soil, and vegetation data (Xia et al., 2012). While GLEAM is forced by global forcing, including Multi-Source Weighted Ensemble Precipitation data (Beck et al., 2017), along with air temperature and radiation from the ERA-Interim (Berrisford et al., 2011). For the seasonal cycle, the ET_{AWB} is characterized by high ET values from June to September, which is
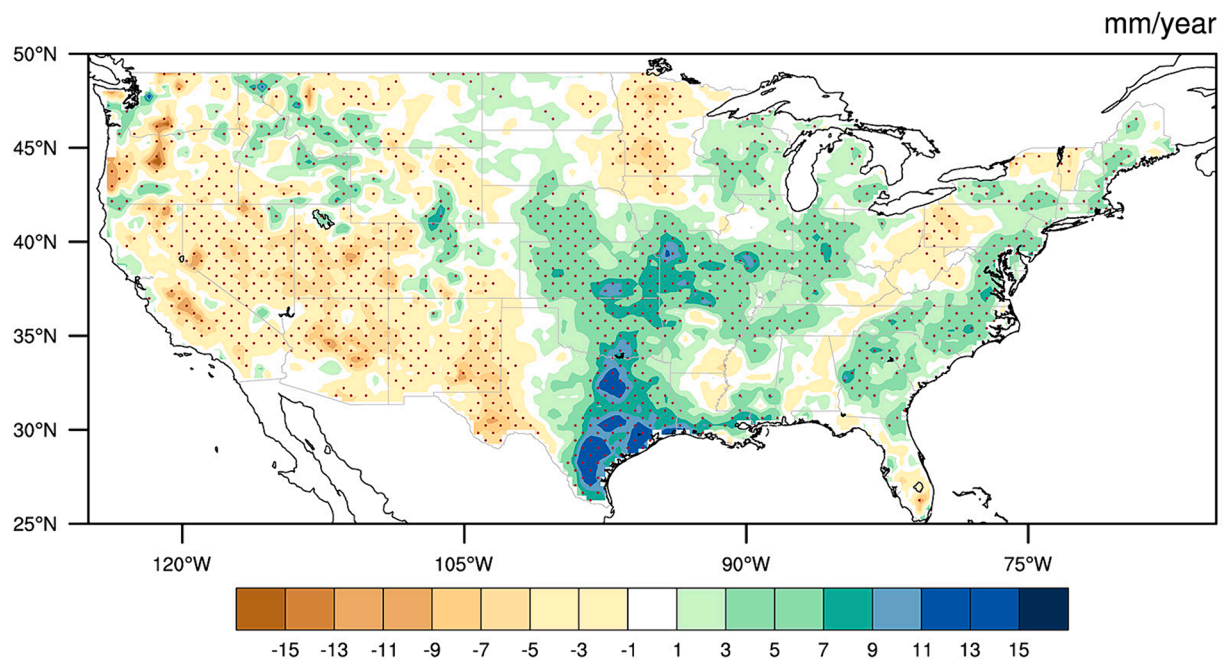
Fig. 9. Spatial pattern of the linear trends in the ET_{AWB} from 1979 to 2021. Dot indicates that linear trend is statistically significant at the 95% confidence level.
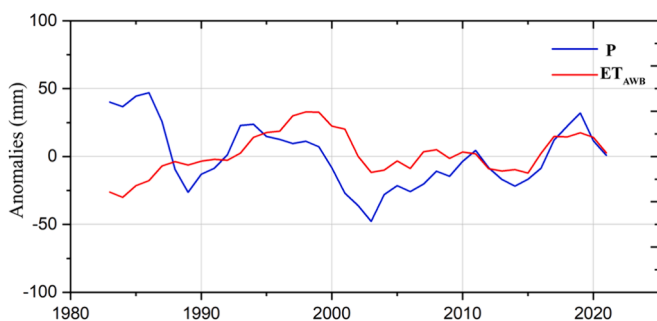

Fig. 10. The CONUS regional ET_{AWB} and precipitation anomaly values from 1979 to 2021, plotted as 5-year moving average values.

inconsistent with other products that show a sudden drop in September (Figure 7 **and** Fig. S2). This may be due to the AWB approach-based ET estimate being constrained by precipitation, and atmospheric water convergence from reanalysis data, while no land surface process related to soil and vegetation is considered. For example, there is a sudden drop in the leaf area index (LAI) in September (Doughty & Goulden, 2009; Wang et al., 2014).

4.2. Uncertainties and implications

The AWB approach employed in this study can be used not only for an independent and mass –conservation-based check for the modeled ET but also to overcome the limitation of the TWB method in basin scale and short time span, providing an ET estimation for a continuous long-time scale on a large spatial scale. However, the accuracy of the AWB approach depends on the quality of the data sources. At the annual scale, the change in the atmospheric water storage in the AWB is negligible. Therefore, the major source of uncertainties comes from precipitation and the integrated atmospheric moisture convergence. In this study, we selected the CPC precipitation data, which has been evaluated over the CONUS (Chen & Xie, 2008; Xie et al., 2010; Wolkeba and Mekonnen, 2024). However, it should be noted that CPC has limitations in accurately representing some grids in mountainous areas due to inadequate

observation station density and difficulty of measurement (Abatzoglou, 2013; Prat & Nelson, 2015). The integrated atmospheric water vapor and moisture convergence are all provided by ERA5 reanalysis (Hersbach et al., 2020). Although previous evaluations have indicated that the ERA5 is indeed more accurate than other atmospheric reanalysis (He et al., 2021; Tarek et al., 2020; Wang et al., 2019), the potential errors in particular forcing are certainly not negligible. Satellite remote sensing technique are also an effective way for detecting atmospheric water vapor (also called precipitable water) (He & Liu, 2019), such as the Precipitable Water Vapor product from the Moderate-resolution Imaging Spectroradiometer (MODIS) Terra platform. For example, the ET estimation for the Tibetan Plateau has used the conjoint AWB and TWB using the precipitable water vapor from MODIS (Li et al., 2019). However, the accuracy of the MODIS product is insufficient and limited under cloudy or hazy weather conditions (King et al., 2003; Prasad & Singh, 2009), which may also introduce additional uncertainties. Nevertheless, changes in the atmospheric water vapor are almost negligible at a monthly to annual scales. Therefore, it does not make much difference to the results of the AWB in this study regardless of the product of atmospheric water vapor product used. It is found that the consistency of the ET_{AWB} and ET_{TWB} is better in the interannual variations in North and South Great Plains (Basins 09–15) but slightly worse in other basins near the ocean or influenced by the monsoon. This may be related to the uncertainties in the atmospheric moisture convergence in the AWB related to extreme tropical cyclones in these areas (Atallah et al., 2007; Mock, 1996). A previous study has shown that ERA5 tends to underestimate strong winds (Chen et al., 2024), therefore leading to an underestimation of the extreme moisture convergence. Continuous long-term satellite observations of wind and specific humidity, which are expected to work in the future, could significantly improve the accuracy of estimated ET. In addition, we only use one type of precipitation and reanalysis data to estimate ET in the present study. Using multiple precipitation and reanalysis could be better accounting for uncertainty.

5. Conclusions

In this study, we estimated long-term 43-year period ET values over the CONUS by the AWB approach from an atmospheric perspective.
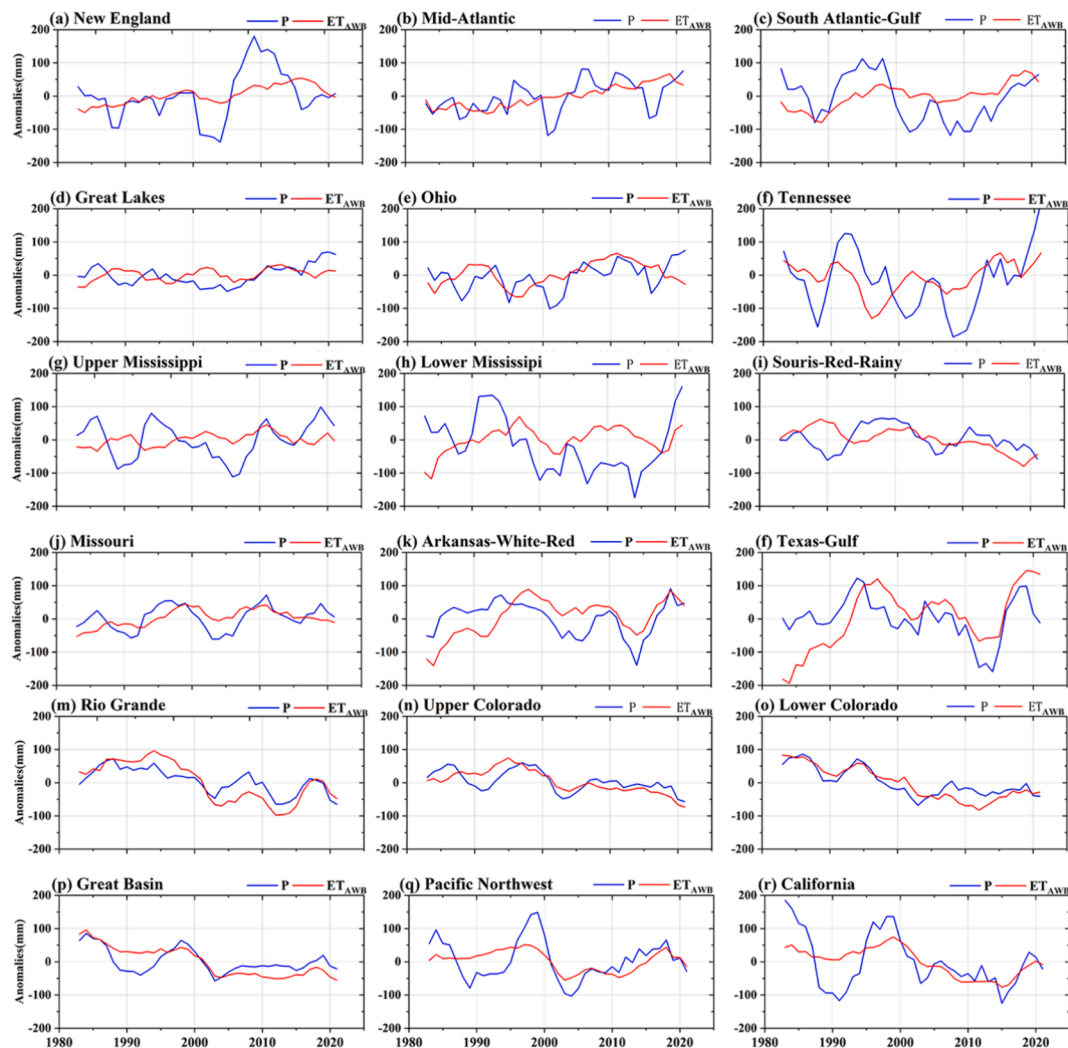
Fig. 11. The ET$_{AWB}$ and precipitation anomaly values in 18 HUC2 basins from 1979 to 2021, plotted as 5-year moving average values.

Evaluations of ET$_{AWB}$ and the other three gridded ET products against the ET$_{TWB}$ at the basin scale indicate that ET$_{AWB}$ performs well in the majority of basins, with R^2 values exceeding 0.8 and NSE values close to 1. Additionally, the estimated ET$_{AWB}$ exhibits comparable interannual variability to the other three products across the CONUS and is also consistent with ET$_{TWB}$ in the majority of the basins.

The multi-year mean ET$_{AWB}$ across the CONUS is 548 ± 26 mm/year. Higher ET$_{AWB}$ values are observed in the southeastern CONUS and the coastal regions of western CONUS, while lower ET values are found in the arid regions of the western CONUS, following the precipitation pattern. For the seasonal cycle, ET$_{AWB}$ shows a maximum in summer and a minimum in winter over the CONUS, capturing the characteristics of the seasonal cycle in different climate zones. During 1979–2021, positive trends are observed in the eastern CONUS, while negative trends are observed in the western CONUS. Inter-comparisons demonstrate that the spatial pattern of multi-year mean and linear trends from the ET$_{AWB}$ are consistent the current main-stream gridded ET products. Additionally, the annual anomalies in the ET$_{AWB}$ and precipitation exhibit high consistency in arid basins, which is expected since these arid regions are water-limited. The AWB approach to estimate ET is a straightforward and simple method to produce a long temporal coverage product for validating regional modeled ET, offering a perspective for gaining further insights. Our results demonstrate that the presented long-term atmospheric water-balanced ET estimates are suitable for regional ET studies and can serve as a reference for modeled regional ET and climate simulations.

CRediT authorship contribution statement

Shasha Shang: Writing – review & editing, Writing – original draft, Visualization, Validation, Software, Methodology, Investigation, Formal analysis, Data curation, Conceptualization. **Gaofeng Zhu:** Writing – review & editing, Supervision, Project administration, Conceptualization. **Kun Zhang:** Writing – review & editing, Data curation. **Huiling Chen:** Writing – review & editing. **Yidong Wang:** Writing – review & editing. **Yang Chen:** Writing – review & editing. **Zhenyu Zhang:** Writing – review & editing. **Ning Ma:** Writing – review & editing, Funding acquisition, Data curation.

Declaration of competing interest

The authors declare that they have no known competing financial interests or personal relationships that could have appeared to influence the work reported in this paper.

Data availability

All data used in this study can be accessed from the website as follows: NLDAS Noah (https://disc.gsfc.nasa.gov/datasets/NLDAS_-NOAH0125_M_002/summary#!); GLEAM (https://www.gleam.eu/

Appendix A. Supplementary data

Supplementary data to this article can be found online at https://doi.org/10.1016/j.jhydrol.2024.131699.

References

Abatzoglou, J.T., 2013. Development of gridded surface meteorological data for ecological applications and modelling. Int. J. Climatol. https://doi.org/10.1002/joc.3413.

Allen, R. G., Pereira, L. S., Howell, T. A., Jensen, M. E. (2011). Evapotranspiration information reporting: I. Factors governing measurement accuracy. In *Agricultural Water Management*. 10.1016/j.agwat.2010.12.015.

Atallah, E., Bosart, L.F., Aiyyer, A.R., 2007. Precipitation distribution associated with landfalling tropical cyclones over the eastern United States. Mon. Weather Rev. https://doi.org/10.1175/MWR3382.1.

Beck, H.E., Van Dijk, A.I.J.M., Levizzani, V., Schellekens, J., Miralles, D.G., Martens, B., De Roo, A., 2017. MSWEP: 3-hourly 0.25° global gridded precipitation (1979–2015) by merging gauge, satellite, and reanalysis data. Hydrol. Earth Syst. Sci. https://doi.org/10.5194/hess-21-589-2017.

Beck, H.E., Zimmermann, N.E., Mcvicar, T.R., Vergopolan, N., Berg, A., Wood, E.F., 2018. Data descriptor: present and future köppen-geiger climate classification maps at 1-km resolution background & summary. Nat. Publ. Group.

Berrisford, P., Kållberg, P., Kobayashi, S., Dee, D., Uppala, S., Simmons, A.J., Poli, P., Sato, H., 2011. Atmospheric conservation properties in ERA-Interim. Q. J. R. Meteorolog. Soc. 137 (659), 1381–1399. https://doi.org/10.1002/qj.864.

Builes-Jaramillo, A., Poveda, G., 2018. Conjoint analysis of surface and atmospheric water balances in the andes-amazon system. Water Resour. Res. https://doi.org/10.1029/2017WR021338.

Chen, T.-C., Collet, F., DiLuca, A., 2024. Evaluation of ERA5 precipitation and 10-m wind speed associated with extratropical cyclones using station data over North America. Int. J. Climatol. 44 (3), 729–747. https://doi.org/10.1002/joc.8339.

Chen, M., Xie, P. (2008). CPC Unified Gauge-Based Analysis of Global Daily Precipitation. *Western Pacific Geophysics Meeting, Cairns, Australia, 29 July - 1 August, 2008*.

Chen, M., Shi, W., Xie, P., Silva, V.B.S., Kousky, V.E., Higgins, R.W., Janowiak, J.E., 2008. Assessing objective techniques for gauge-based analyses of global daily precipitation. Journal of Geophysical Research Atmospheres. https://doi.org/10.1029/2007JD009132.

Chen, H., Zhu, G., Zhang, K., Bi, J., Jia, X., Ding, B., Zhang, Y., Shang, S., Zhao, N., Qin, W., 2020. Evaluation of evapotranspiration models using different LAI and meteorological forcing data from 1982 to 2017. Remote Sens. (Basel) 12 (15). https://doi.org/10.3390/RS12152473.

Cui, W., Dong, X., Xi, B., Kennedy, A., 2017. Evaluation of reanalyzed precipitation variability and trends using the gridded gauge-based analysis over the CONUS. J. Hydrometeorol. https://doi.org/10.1175/JHM-D-17-0029.1.

Dagan, G., Stier, P., Watson-Parris, D., 2019. Analysis of the atmospheric water budget for elucidating the spatial scale of precipitation changes under climate change. Geophys. Res. Lett. https://doi.org/10.1029/2019GL084173.

Doughty, C.E., Goulden, M.L., 2009. Seasonal patterns of tropical forest leaf area index and CO2 exchange. J. Geophys. Res. Biogeo. https://doi.org/10.1029/2007JG000590.

Gelaro, R., McCarty, W., Suárez, M.J., Todling, R., Molod, A., Takacs, L., Randles, C.A., Darmenov, A., Bosilovich, M.G., Reichle, R., Wargan, K., Coy, L., Cullather, R., Draper, C., Akella, S., Buchard, V., Conaty, A., da Silva, A.M., Gu, W., Zhao, B., 2017. The modern-era retrospective analysis for research and applications, version 2 (MERRA-2). J. Clim. https://doi.org/10.1175/JCLI-D-16-0758.1.

Gershunov, A., Shulgina, T., Clemesha, R.E.S., Guirguis, K., Pierce, D.W., Dettinger, M.D., Lavers, D.A., Cayan, D.R., Polade, S.D., Kalansky, J., Ralph, F.M., 2019. Precipitation regime change in Western North America: the role of Atmospheric Rivers. Sci. Rep. https://doi.org/10.1038/s41598-019-46169-w.

Hamlet, A.F., Mote, P.W., Clark, M.P., Lettenmaier, D.P., 2007. Twentieth-century trends in runoff, evapotranspiration, and soil moisture in the western United States. J. Clim. https://doi.org/10.1175/JCLI4051.1.

He, J., Liu, Z., 2019. Comparison of satellite-derived precipitable water vapor through near-infrared remote sensing channels. IEEE Trans. Geosci. Remote Sens. https://doi.org/10.1109/TGRS.2019.2932847.

He, Y., Wang, K., Feng, F., 2021. Improvement of ERA5 over ERA-interim in simulating surface incident solar radiation throughout China. J. Clim. https://doi.org/10.1175/JCLI-D-20-0300.1.

Hersbach, H., Bell, B., Berrisford, P., Hirahara, S., Horányi, A., Muñoz-Sabater, J., Nicolas, J., Peubey, C., Radu, R., Schepers, D., Simmons, A., Soci, C., Abdalla, S., Abellan, X., Balsamo, G., Bechtold, P., Biavati, G., Bidlot, J., Bonavita, M., Thépaut, J.N., 2020. The ERA5 global reanalysis. Q. J. R. Meteorolog. Soc. https://doi.org/10.1002/qj.3803.

Humphrey, V., Gudmundsson, L., 2019. GRACE-REC: a reconstruction of climate-driven water storage changes over the last century. Earth Syst. Sci. Data. https://doi.org/10.5194/essd-11-1153-2019.

Jung, M., Reichstein, M., Margolis, H.A., Cescatti, A., Richardson, A.D., Arain, M.A., Arneth, A., Bernhofer, C., Bonal, D., Chen, J., Gianelle, D., Gobron, N., Kiely, G., Kutsch, W., Lasslop, G., Law, B.E., Lindroth, A., Merbold, L., Montagnani, L., Williams, C., 2011. Global patterns of land-atmosphere fluxes of carbon dioxide, latent heat, and sensible heat derived from eddy covariance, satellite, and meteorological observations. J. Geophys. Res. Biogeo. https://doi.org/10.1029/2010JG001566.

Jung, M., Koirala, S., Weber, U., Ichii, K., Gans, F., Camps-Valls, G., Papale, D., Schwalm, C., Tramontana, G., Reichstein, M., 2019. The FLUXCOM ensemble of global land-atmosphere energy fluxes. Sci. Data. https://doi.org/10.1038/s41597-019-0076-8.

King, M.D., Menzel, W.P., Kaufman, Y.J., Tanré, D., Gao, B.C., Platnick, S., Ackerman, S. A., Remer, L.A., Pincus, R., Hubanks, P.A., 2003. Cloud and aerosol properties, precipitable water, and profiles of temperature and water vapor from MODIS. IEEE Trans. Geosci. Remote Sens. https://doi.org/10.1109/TGRS.2002.808226.

Kobayashi, S., Ota, Y., Harada, Y., Ebita, A., Moriya, M., Onoda, H., Onogi, K., Kamahori, H., Kobayashi, C., Endo, H., Miyaoka, K., Kiyotoshi, T., 2015. The JRA-55 reanalysis: general specifications and basic characteristics. J. Meteorol. Soc. Jpn. https://doi.org/10.2151/jmsj.2015-001.

Koster, R.D., Salvucci, G.D., Rigden, A.J., Jung, M., Collatz, G.J., Schubert, S.D., 2015. The pattern across the continental United States of evapotranspiration variability associated with water availability. Front. Earth Sci. https://doi.org/10.3389/feart.2015.00035.

Li, X., Long, D., Han, Z., Scanlon, B.R., Sun, Z., Han, P., Hou, A., 2019. Evapotranspiration estimation for tibetan plateau headwaters using conjoint terrestrial and atmospheric water balances and multisource remote sensing. Water Resour. Res. https://doi.org/10.1029/2019WR025196.

Liu, W., Wang, L., Zhou, J., Li, Y., Sun, F., Fu, G., Li, X., Sang, Y.F., 2016. A worldwide evaluation of basin-scale evapotranspiration estimates against the water balance method. J. Hydrol. https://doi.org/10.1016/j.jhydrol.2016.04.006.

Liu, H., Xin, X., Su, Z., Zeng, Y., Lian, T., Li, L., Yu, S., Zhang, H., 2023. Intercomparison and evaluation of ten global ET products at site and basin scales. J. Hydrol. https://doi.org/10.1016/j.jhydrol.2022.128887.

Liu, J., You, Y., Li, J., Sitch, S., Gu, X., Nabel, J.E.M.S., Lombardozzi, D., Luo, M., Feng, X., Arneth, A., Jain, A.K., Friedlingstein, P., Tian, H., Poulter, B., Kong, D., 2021a. Response of global land evapotranspiration to climate change, elevated CO2, and land use change. Agric. For. Meteorol. https://doi.org/10.1016/j.agrformet.2021.108663.

Liu, J., Zhang, J., Kong, D., Feng, X., Feng, S., Xiao, M., 2021b. Contributions of anthropogenic forcings to evapotranspiration changes over 1980–2020 using GLEAM and CMIP6 simulations. J. Geophys. Res. Atmos. https://doi.org/10.1029/2021JD035367.

Long, D., Longuevergne, L., Scanlon, B.R., 2014. Uncertainty in evapotranspiration from land surface modeling, remote sensing, and GRACE satellites. Water Resour. Res. https://doi.org/10.1002/2013WR014581.

Longuevergne, L., Scanlon, B. R., Wilson, C. R. (2010). GRACE hydrological estimates for small basins: Evaluating processing approaches on the High Plains aquifer, USA. *Water Resources Research*. 10.1029/2009WR008564.

Lu, Y., Steele-Dunne, S.C., Farhadi, L., van de Giesen, N., 2017. Mapping surface heat fluxes by assimilating SMAP soil moisture and GOES land surface temperature data. Water Resour. Res. https://doi.org/10.1002/2017WR021415.

Ma, N., Zhang, Y., 2022. Increasing Tibetan Plateau terrestrial evapotranspiration primarily driven by precipitation. Agric. For. Meteorol. https://doi.org/10.1016/j.agrformet.2022.108887.

Ma, N., Niu, G.Y., Xia, Y., Cai, X., Zhang, Y., Ma, Y., Fang, Y., 2017. A systematic evaluation of noah-MP in simulating land-atmosphere energy, water, and carbon exchanges over the continental United States. J. Geophys. Res. Atmos. https://doi.org/10.1002/2017JD027597.

Ma, N., Szilagyi, J., 2019. The CR of evaporation: a calibration-free diagnostic and benchmarking tool for large-scale terrestrial evapotranspiration modeling. Water Resour. Res. https://doi.org/10.1029/2019WR024867.

Ma, N., Szilagyi, J., Jozsa, J., 2020. Benchmarking large-scale evapotranspiration estimates: a perspective from a calibration-free complementary relationship approach and FLUXCOM. J. Hydrol. https://doi.org/10.1016/j.jhydrol.2020.125221.

Ma, N., Szilagyi, J., Zhang, Y., 2021. Calibration-free complementary relationship estimates terrestrial evapotranspiration globally. Water Resour. Res. https://doi.org/10.1029/2021WR029691.

Ma, N., Zhang, Y., Szilagyi, J., 2024. Water-balance-based evapotranspiration for 56 large river basins: A benchmarking dataset for global terrestrial evapotranspiration modeling. J. Hydrol. 630, 130607. https://doi.org/10.1016/j.jhydrol.2024.130607.

Martens, B., Miralles, D.G., Lievens, H., Van Der Schalie, R., De Jeu, R.A.M., Fernández-Prieto, D., Beck, H.E., Dorigo, W.A., Verhoest, N.E.C., 2017a. GLEAM v3: satellite-based land evaporation and root-zone soil moisture. Geosci. Model Dev. 10 (5), 1903–1925. https://doi.org/10.5194/gmd-10-1903-2017.

Martens, B., Miralles, D.G., Lievens, H., Van Der Schalie, R., De Jeu, R.A.M., Fernández-Prieto, D., Beck, H.E., Dorigo, W.A., Verhoest, N.E.C., 2017b. GLEAM v3: satellite-based land evaporation and root-zone soil moisture. Geosci. Model Dev. https://doi.org/10.5194/gmd-10-1903-2017.

Masson, V., Champeaux, J.L., Chauvin, F., Meriguet, C., Lacaze, R., 2003. A global database of land surface parameters at 1-km resolution in meteorological and climate models. J. Clim. https://doi.org/10.1175/1520-0442-16.9.1261.

Miralles, D.G., Jiménez, C., Jung, M., Michel, D., Ershadi, A., Mccabe, M.F., Hirschi, M., Martens, B., Dolman, A.J., Fisher, J.B., Mu, Q., Seneviratne, S.I., Wood, E.F., Fernández-Prieto, D., 2016. The WACMOS-ET project - Part 2: evaluation of global terrestrial evaporation data sets. Hydrol. Earth Syst. Sci. https://doi.org/10.5194/hess-20-823-2016.

Mock, C.J., 1996. Climatic controls and spatial variations of precipitation in the western United States. J. Clim. https://doi.org/10.1175/1520-0442(1996)009<1111:ccasvo>2.0.co;2.

Mu, Q., Zhao, M., Running, S.W., 2011. Improvements to a MODIS global terrestrial evapotranspiration algorithm. Remote Sens. Environ. https://doi.org/10.1016/j.rse.2011.02.019.

Mueller, B., Hirschi, M., Jimenez, C., Ciais, P., Dirmeyer, P.A., Dolman, A.J., Fisher, J.B., Jung, M., Ludwig, F., Maignan, F., Miralles, D.G., McCabe, M.F., Reichstein, M., Sheffield, J., Wang, K., Wood, E.F., Zhang, Y., Seneviratne, S.I., 2013. Benchmark products for land evapotranspiration: LandFlux-EVAL multi-data set synthesis. Hydrol. Earth Syst. Sci. https://doi.org/10.5194/hess-17-3707-2013.

Oki, T., Kanae, S., 2006. Global hydrological cycles and world water resources. In Sci. https://doi.org/10.1126/science.1128845.

Oki, T., Musiake, K., Matsuyama, H., Masuda, K., 1995. Global atmospheric water balance and runoff from large river basins. Hydrol. Process. https://doi.org/10.1002/hyp.3360090513.

Pascolini-Campbell, M.A., Reager, J.T., Fisher, J.B., 2020. GRACE-based mass conservation as a validation target for basin-scale evapotranspiration in the contiguous United States. Water Resour. Res. https://doi.org/10.1029/2019WR026594.

Portmann, R.W., Solomon, S., Hegerl, G.C., 2009. Spatial and seasonal patterns in climate change, temperatures, and precipitation across the United States. In: Proceedings of the National Academy of Sciences of the United States of America. https://doi.org/10.1073/pnas.0808533106.

Prasad, A.K., Singh, R.P., 2009. Validation of MODIS Terra, AIRS, NCEP/DOE AMIP-II Reanalysis-2, and AERONET Sun photometer derived integrated precipitable water vapor using ground-based GPS receivers over India. Journal of Geophysical Research Atmospheres. https://doi.org/10.1029/2008JD011230.

Prat, O.P., Nelson, B.R., 2015. Evaluation of precipitation estimates over CONUS derived from satellite, radar, and rain gauge data sets at daily to annual scales (2002–2012). Hydrol. Earth Syst. Sci. https://doi.org/10.5194/hess-19-2037-2015.

Rasmusson, E.M., 1968. Atmospheric water vapor transport and the water balance of north america. Mon. Weather Rev. https://doi.org/10.1175/1520-0493(1968)096<0720:awvtat>2.0.co;2.

Rasmusson, E.M., 1971. A study of the hydrology of eastern north america using atmospheric vapor flux data. Mon. Weather Rev. https://doi.org/10.1175/1520-0493(1971)099<0119:asotho>2.3.co;2.

Reitz, M., Sanford, W.E., Saxe, S., 2023. Ensemble Estimation of Historical Evapotranspiration for the Conterminous U.S. Water Resour. Res. https://doi.org/10.1029/2022WR034012.

Rodell, M., Famiglietti, J.S., Chen, J., Seneviratne, S.I., Viterbo, P., Holl, S., Wilson, C.R., 2004. Basin scale estimates of evapotranspiration using GRACE and other observations. Geophys. Res. Lett. https://doi.org/10.1029/2004GL020873.

Ropelewski, C.F., Yarosh, E.S., 1998. The observed mean annual cycle of moisture budgets over the central United States (1973–92). J. Clim. https://doi.org/10.1175/1520-0442(1998)011<2180:TOMACO>2.0.CO;2.

Seaber, P.R., Kapinos, F.P., Knapp, G.L., 1987. Hydrologic unit maps (USA). US Geological Survey Water-Supply Paper.

Shang, S., Arnault, J., Zhu, G., Chen, H., Wei, J., Zhang, K., Zhang, Z., Laux, P., Kunstmann, H., 2022. Recent increase of spring precipitation over the three-river headwaters region—water budget analysis based on global reanalysis (ERA5) and ET-tagging extended regional climate modeling. J. Clim. https://doi.org/10.1175/JCLI-D-21-0829.1.

Shao, X., Zhang, Y., Liu, C., Chiew, F.H.S., Tian, J., Ma, N., Zhang, X., 2022. Can indirect evaluation methods and their fusion products reduce uncertainty in actual evapotranspiration estimates? Water Resour. Res. https://doi.org/10.1029/2021WR031069.

Su, Y., Smith, J.A., 2021. An atmospheric water balance perspective on extreme rainfall potential for the contiguous US. Water Resour. Res. https://doi.org/10.1029/2020WR028387.

Szilagyi, J., Crago, R., Qualls, R., 2017. A calibration-free formulation of the complementary relationship of evaporation for continental-scale hydrology. J. Geophys. Res. https://doi.org/10.1002/2016JD025611.

Szilagyi, J., Jozsa, J., 2018. Evapotranspiration trends (1979–2015) in the central valley of California, USA: contrasting tendencies during 1981–2007. Water Resour. Res. https://doi.org/10.1029/2018WR022704.

Tapley, B.D., Watkins, M.M., Flechtner, F., Reigber, C., Bettadpur, S., Rodell, M., Sasgen, I., Famiglietti, J.S., Landerer, F.W., Chambers, D.P., Reager, J.T., Gardner, A. S., Save, H., Ivins, E.R., Swenson, S.C., Boening, C., Dahle, C., Wiese, D.N., Dobslaw, H., Velicogna, I., 2019. Contributions of GRACE to understanding climate change. In Nature Climate Change. https://doi.org/10.1038/s41558-019-0456-2.

Tarek, M., Brissette, F.P., Arsenault, R., 2020. Evaluation of the ERA5 reanalysis as a potential reference dataset for hydrological modelling over North America. Hydrol. Earth Syst. Sci. https://doi.org/10.5194/hess-24-2527-2020.

Trenberth, K.E., Fasullo, J.T., Kiehl, J., 2009. Earth's global energy budget. Bull. Am. Meteorol. Soc. https://doi.org/10.1175/2008BAMS2634.1.

Velpuri, N.M., Senay, G.B., Singh, R.K., Bohms, S., Verdin, J.P., 2013. A comprehensive evaluation of two MODIS evapotranspiration products over the conterminous United States: Using point and gridded FLUXNET and water balance ET. Remote Sens. Environ. https://doi.org/10.1016/j.rse.2013.07.013.

Volk, J.M., Huntington, J., Melton, F.S., Allen, R., Anderson, M.C., Fisher, J.B., Kilic, A., Senay, G., Halverson, G., Knipper, K., Minor, B., Pearson, C., Wang, T., Yang, Y., Evett, S., French, A.N., Jasoni, R., Kustas, W., 2023. Development of a benchmark eddy flux evapotranspiration dataset for evaluation of satellite-driven evapotranspiration models over the CONUS. Agric. For. Meteorol. https://doi.org/10.1016/j.agrformet.2023.109307.

Wang, L., Good, S.P., Caylor, K.K., 2014. Global synthesis of vegetation control on evapotranspiration partitioning. Geophys. Res. Lett. https://doi.org/10.1002/2014GL061439.

Wang, C., Graham, R.M., Wang, K., Gerland, S., Granskog, M.A., 2019. Comparison of ERA5 and ERA-Interim near-surface air temperature, snowfall and precipitation over Arctic sea ice: effects on sea ice thermodynamics and evolution. Cryosphere 13 (6), 1661–1679. https://doi.org/10.5194/tc-13-1661-2019.

Wolkeba, T., Mekonnen, M., 2024. Evaluation of gridded precipitation data in water availability modeling in CONUS. J. Hydrol. 628, 130575. https://doi.org/10.1016/j.jhydrol.2023.130575.

Xia, Y., Mitchell, K., Ek, M., Sheffield, J., Cosgrove, B., Wood, E., Luo, L., Alonge, C., Wei, H., Meng, J., Livneh, B., Lettenmaier, D., Koren, V., Duan, Q., Mo, K., Fan, Y., Mocko, D., 2012. Continental-scale water and energy flux analysis and validation for the North American Land Data Assimilation System project phase 2 (NLDAS-2): 1. Intercomparison and application of model products. J. Geophys. Res. Atmos. 117 (3) https://doi.org/10.1029/2011JD016048.

Xia, Y., Cosgrove, B.A., Mitchell, K.E., Peters-Lidard, C.D., Ek, M.B., Brewer, M., Mocko, D., Kumar, S.V., Wei, H., Meng, J., Luo, L., 2016. Basin-scale assessment of the land surface water budget in the national centers for environmental prediction operational and research NLDAS-2 systems. J. Geophys. Res. https://doi.org/10.1002/2015JD023733.

Xie, P., Chen, M., Shi, W., 2010. CPC global unified gauge-based analysis of daily precipitation. Amer. Meteor. Soc.

Xu, T., Guo, Z., Xia, Y., Ferreira, V.G., Liu, S., Wang, K., Yao, Y., Zhang, X., Zhao, C., 2019. Evaluation of twelve evapotranspiration products from machine learning, remote sensing and land surface models over conterminous United States. J. Hydrol. https://doi.org/10.1016/j.jhydrol.2019.124105.

Xu, C.Y., Singh, V.P., 2005. Evaluation of three complementary relationship evapotranspiration models by water balance approach to estimate actual regional evapotranspiration in different climatic regions. J. Hydrol. https://doi.org/10.1016/j.jhydrol.2004.10.024.

Yang, Y., Long, D., Shang, S., 2013. Remote estimation of terrestrial evapotranspiration without using meteorological data. Geophys. Res. Lett. https://doi.org/10.1002/grl.50450.

Yeh, P.J.F., Irizarry, M., Eltahir, E.A.B., 1998. Hydroclimatology of Illinois: a comparison of monthly evaporation estimates based on atmospheric water balance and soil water balance. In J. Geophysical Res. Atmospheres. https://doi.org/10.1029/98JD01721.

Yu, L., Qiu, G.Y., Yan, C., Zhao, W., Zou, Z., Ding, J., Qin, L., Xiong, Y., 2022. A global terrestrial evapotranspiration product based on the three-temperature model with fewer input parameters and no calibration requirement. Earth Syst. Sci. Data. https://doi.org/10.5194/essd-14-3673-2022.

Zhang, Y., Chiew, F.H.S., Peña-Arancibia, J., Sun, F., Li, H., Leuning, R., 2017. Global variation of transpiration and soil evaporation and the role of their major climate drivers. J. Geophys. Res. Atmos. 122, 6868–6881. https://doi.org/10.1002/2017JD027025.

Zhang, K., Zhu, G., Ma, J., Yang, Y., Shang, S., Gu, C., 2019. Parameter analysis and estimates for the MODIS evapotranspiration algorithm and multiscale verification. Water Resour. Res. 55 (3), 2211–2231. https://doi.org/10.1029/2018WR023485.

Zhang, K., Zhu, G., Ma, N., Chen, H., Shang, S., 2022. Improvement of evapotranspiration simulation in a physically based ecohydrological model for the groundwater–soil–plant–atmosphere continuum. J. Hydrol. https://doi.org/10.1016/j.jhydrol.2022.128440.

Zou, L., Zhan, C., Xia, J., Wang, T., Gippel, C.J., 2017. Implementation of evapotranspiration data assimilation with catchment scale distributed hydrological model via an ensemble Kalman Filter. J. Hydrol. https://doi.org/10.1016/j.jhydrol.2017.04.036.